Confinement Studies of Helical-axis Heliotron Plasmas

F. Sano 1), T. Mizuuchi 1), K. Kondo 2), K. Nagasaki 1), H. Okada 1), S. Kobayashi 1), K. Hanatani 1), Y. Nakamura 2), S. Yamamoto 1), Y. Torii 1), Y. Suzuki 2), H. Shidara 2), H. Kawazome 2), M. Kaneko 2), H. Arimoto 2), T. Azuma 2), J. Arakawa 2) , K. Ohashi 2), M. Kikutake 2), N. Shimazaki 2), T. Hamagami 2), G. Motojima 2), H. Yamazaki 2), M. Yamada 2), H. Kitagawa 2), T. Tsuji 2), H. Nakamura 2), S. Watanabe 2), S. Murakami 3), N. Nishino 4), M.Yokoyama 5), Y. Ijiri 1), T. Senju 1), K. Yaguchi 1), K. Sakamoto 1), K. Tohshi 1), M. Shibano 1), V. Tribaldos 6), V.V.Chechkin 7)

1) Institute of Advanced Energy, Kyoto University, Gokashou, Uji, Japan
2) Graduate School of Energy Science, Kyoto University, Kyoto, Japan
3) Graduate School of Engineering, Kyoto University, Kyoto, Japan
4) Graduate School of Engineering, Hiroshima University, Hiroshima, Japan
5) National Institute for Fusion Science, Toki, Gifu, Japan
6) Laboratorio Nacional de Fusion, Asociacion EURATOM-CIEMAT, Madrid, Spain
7) Institute of Plasma Physics, NSC KIPT, 61108 Kharkov, Ukraine

e-mail contact of main author: sano@iae.kyoto-u.ac.jp

Abstract. The L-H transition in the helical-axis heliotron, Heliotron J, was investigated. For ECH-only, NBI-only and ECH+NBI combination heating plasmas, the confinement quality of the H-mode was examined with special regard to the magnetic configuration, the vacuum edge iota value of which was chosen as a label of the configuration. The experimental iota dependence of the H_{ISS95}-factor ($\tau_E^{exp}/\tau_E^{ISS95}$) has revealed that there exist the specific configurations for which the high-quality H-modes ($1.3< H_{ISS95} <1.8$) are attained. These iota ranges are located to be slightly less than the major natural resonances of Heliotron J, i.e., n/m=4/8, 4/7 and 12/22. As an attempt to understand this configuration dependence, the configuration dependence of the geometrical poloidal viscous damping rate coefficient, C_p, was calculated and compared with the experiment. Edge plasma characteristics are also measured and discussed with regard to the E_r-shear formation at the transition.

1. Introduction

In September 2002, the first experimental findings of the spontaneous transitions to a state of improved particle and energy confinement in Heliotron J were obtained with electron cyclotron heating (ECH) of 70 GHz, 0.3 MW and 0.1 s, the launching port of which was the horizontal port located at one of the four corner sections of Heliotron J [1, 2]. The observed spontaneous transitions for hydrogen plasmas had many of the characteristic signatures of L-H transition such as a sudden drop of H_α emission, coupled with monotonic increases in plasma density ($\bar{n}_e$) and in plasma energy content (W_p^{diam}) in the time scale of energy confinement time (τ_E^{exp}). While the H-mode confinement improvement was transitory in nature, the magnetic topology windows for achieving these transitions ($0.54< \iota(a)/2\pi <0.56$ in separatrix discharge and $0.62< \iota(a)/2\pi <0.63$ in partial wall-limiter discharge, where $\iota(a)/2\pi$ is the vacuum edge iota value) at the fixed ECH power of 0.3 MW were narrow and isolated in the scanning iota range, where the auxiliary vertical field coil current was varied to change the iota. It was also found that there was a threshold of line-averaged density ($\bar{n}_e$=1.2~1.6×10^{19} m^{-3}) below which the H-mode transition could not be obtained [3]. The increase in plasma energy content $\Delta W_p^{diam}/W_p^{diam}$ in the 0.3-MW ECH H-mode reached about 70% in the separatrix discharge and the estimated energy confinement time τ_E^{exp} was found to be enhanced beyond the normal ISS95 scaling [4], being 50% longer than that in the before transition phase. Furthermore, by using a tangential H^0 neutral beam of 28 keV and 0.6

MW, the similar H-mode results of NBI heated plasmas were studied and discussed in Ref. [5,6]. However, the systematic studies of the H-mode confinement quality with special regard to the magnetic configuration remained to be done [7]. From the database collected thereafter including deuterium ECH plasmas, it is found that the H-mode transitions in Heliotron J behave, in some degree, similarly to those of tokamaks, but the obtained confinement enhancement factor (H_{ISS95}-factor) over the L-mode (ISS95) confinement remains to be a relatively low value of less than 2 and there is some evidence that their confinement qualities behave differently depending on the magnetic configuration. The crucial role of the magnetic configuration at the H-mode transition as well as during the evolution of the H-mode is expected to be that of controlling the different driving and damping mechanisms of the plasma flows (or radial electric fields) especially in the plasma boundary region. The neoclassical (e.g., ion orbit losses) or anomalous mechanisms (e.g., Stringer spin-up, Reynolds stress) are proposed as the candidates to provide the driving terms. The charge-exchange momentum losses, parallel viscosity (magnetic pumping), or turbulent viscosity are considered to provide the damping terms. The specific structure of the $|B|$ spectrum on the boundary magnetic surface is expected to play an important role at the H-mode transition through viscous damping or magnetic pumping. The edge magnetic topology in itself is also an important factor which controls neutral gas density through plasma-wall interactions. Therefore, it is interesting to investigate the configuration dependence of the H-mode confinement quality from the viewpoint of the anomalous transport optimization of the helical-axis heliotron. Thus, one of the key issues being addressed in the H-mode research in the 2004 experimental campaign was the exploration of the specific magnetic configuration required for the enhancement of its H-mode performance.

2. Experimental Set-up

Heliotron J is a medium-sized helical-axis heliotron device with major radius R=1.2 m, average plasma minor radius a = 0.1-0.2 m and magnetic field strength on its magnetic axis B_0 <1.5 T [8-10]. Its coil set can provide considerable flexibility toward the configuration control of a helical-axis heliotron plasma [11]. In the 2003 campaign, a 30-keV, 0.6-MW NBI system and a 20-MHz, 0.5-MW ion cyclotron range of frequency (ICRF) heating system were installed in Heliotron J for ion heating and high β plasma production. In order to install the ICRF antennas, the ECH launching position was altered from the horizontal port for horizontal microwave injection into the top port for its vertical injection. Therefore, the H-mode physics experiments with regard to the magnetic topology control have been carried out by changing the ratio of the helical field coil current to the toroidal field coil currents in order that the magnetic axis position should be nearly kept constant, where the edge iota can be changed from 0.49 to 0.65. The working gas for the target ECH plasmas has been changed from hydrogen to deuterium in the 2003-2004 campaign. The details of the 70GHz ECH system are described in Ref. [12]. The injected power is up to 0.4 MW, and the pulse length is up to 0.1 s in the experiment. The Gaussian beam diameter of the second harmonic X-mode is 120 mm at the magnetic axis, which is about a half of the plasma diameter on the equatorial plane. The ECH power absorption efficiency was estimated by using TRECE code [13] while taking into account the assumed 30% multireflection effects. The NBI power absorption efficiency was estimated by using the model simulation results of the Monte-Carlo HELIOS code [14]. As for the details of the NBI system and ICRF system, see Ref. [9]. The diagnostics such as microwave interferometer, diamagnetic loops, visible light monitors, H_α/D_α emission detectors, AXUV diodes, Langmuir probe array located in the SOL, soft X-ray detectors, ECE monitors and so on are used to measure the confinement characteristics of the plasma.

3. Description of Different H-mode Transition Experiments

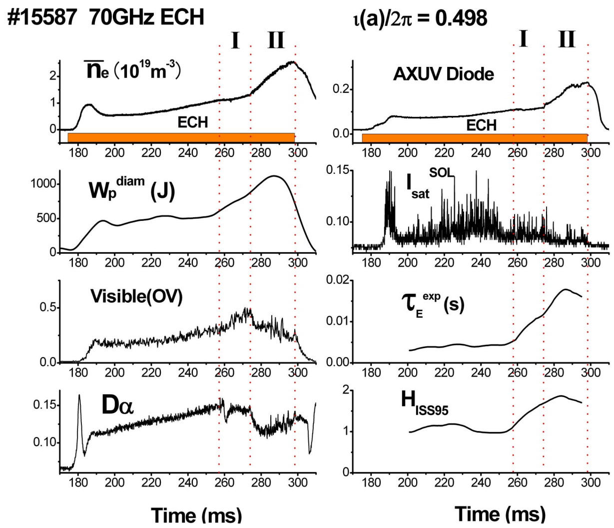

FIG.1. Time evolution of the line-averaged electron density $\bar{n}_e$, diamagnetic plasma energy content W_p^{diam}, visible light signal (Oxygen V), D_α signal, AXUV diode signal, electrostatic probe signal I_s, experimental energy confinement time τ_E^{exp} and H_{ISS95}-factor for ECH(D^+)-only plasma at $\iota(a)/2\pi$=0.49.

3.1. H-mode Transition of ECH (D^+)-only Plasma

With regard to the H-mode transition, two types of transitions are actually observed: a single-step L-H transition and repetitive L-H-L transition sequences. The latter type is, in fact, more common. Figure 1 shows a typical temporal development of an H-mode transition occurring in the ECH pulse at the vacuum edge iota of 0.49 in the 2004 campaign. At a given ECH power of 0.14 MW, the discharge dynamics is controlled by gas puffing and normally the H-mode transition appears spontaneously after the strong gas puffing or during the constant gas puffing. Depending on the density evolution, the ECH discharge gradually develops into H-mode, characterized by the appearance of the L-H-L short-lived repetitive transition (or dithering) signal of D_α indicating the threshold behaviour (Phase I). At the timing of 273 ms, the final, and established H-mode is achieved when the strong and long-lived drop of D_α takes place accompanied by a marked increase in $d\bar{n}_e/dt$ up to ~5×10^{20} $m^{-3}s^{-1}$ (Phase II). It is noted that, although a marked increase in $d\bar{n}_e/dt$ starts in Phase II, the increase in dW_p^{diam}/dt already starts in Phase I. The maximum increment in W_p^{diam} reaches about 100% throughout Phases I and II. The lack of the density control in Phase II means that the H-mode is self-terminating due to radiation collapse. The ECH H-mode termination events seem to fall into two groups: one is the low-density termination ($\bar{n}_e< 2\times10^{19}m^{-3}$) which is often observed at the back transition in the single-step transition and the other is the high-density termination ($\bar{n}_e>2\times10^{19}m^{-3}$) which leads to radiation collapse. A candidate mechanism for the latter type of termination is the ECH cut-off at the central electron densities over $3\times10^{19}m^{-3}$. The ray tracing calculation of 70-GHz ECH power absorption in the case of the top launch expects a drastic drop of the absorption efficiency down to less than 50% at line-averaged densities over 2×10^{19} m^{-3} while it remains over 80% in the line-averaged density range of 0.5 to 1.5 $\times10^{19}$ m^{-3} under the assumptions of the flat density profile and the parabolic temperature profile (Te(0)=500 eV). Therefore, the transient nature of the ECH-only H-mode at high densities may be interpreted as being due to a direct result of the reduced coupling of the ECH power into the plasma. The AXUV diode signal shows an increase in Phase II, but the possibility of strong impurity accumulation due to the enhanced bulk particle confinement is limited from its comparison with the rise rate of line-averaged density. The experimental peak energy confinement time τ_E^{exp} of 18 ms, which is typically obtained earlier than the peak plasma energy content, corresponds to the H_{ISS95}-factor of ~1.8, with that of ~1 prior to the transition of Phase I. The low-frequency D_α fluctuations during H-mode such as edge localized modes (ELMs) are not observed in this plasma, although some bursts or sharp spikes can be seen as the edge activities. The D_α spikes are found to be coordinated with the SOL density signals, I_s, measured by the movable

Langmuir probe array located in the SOL region. Compared with the ECH (H^+)-only plasmas in the 2002 campaign, there seems to be no significant difference in the transition behaviour between hydrogen and deuterium.

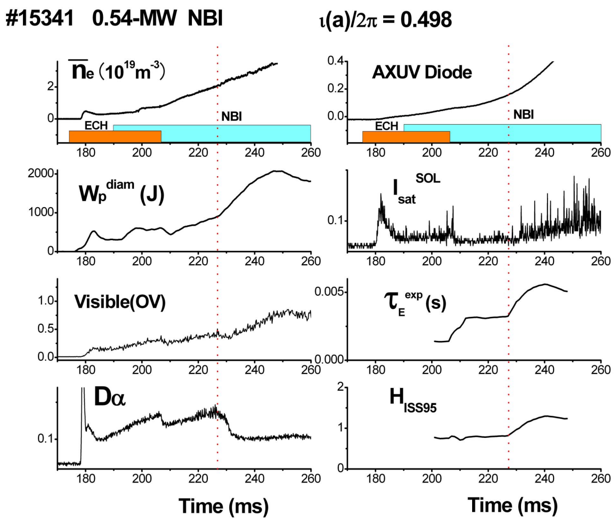

FIG. 2. Time evolution of the key plasma parameters for NBI(H^0)-only plasma at $\iota(a)/2\pi$=0.49.

3.2. H-mode Transition of NBI ($H^0 \rightarrow D^+$)-only Plasma

An example of the NBI-only H-mode transition is shown in Fig.2 where the 28 keV neutral beam of 0.54 MW (BL-2) is injected tangentially into the ECH (D^+) plasma and then the plasma is maintained only by NBI after ECH turn-off. During the initial ECH and ECH+NBI phases, the D_α signal shows a comparatively high intensity due to the particle pump-out caused by ECH while it shows a drop after ECH turn-off at the timing of 207 ms, resulting in the improved particle confinement time. During the subsequent NBI-only phase, the D_α signal again starts to gradually drop at the timing of 228 ms, followed by a sharp, a factor of 2 drop at the timing of 230 ms when the established ELM-free H-mode is reached. After this H-mode transition, the increase in $d\bar{n}_e/dt$ is modest whereas the increase in dW_p^{diam}/dt is notable. The energy confinement time τ_E^{exp} increases at the transition, manifesting a discontinuity in dW_p^{diam}/dt. The peak τ_E^{exp} of 6 ms corresponds to the H_{ISS95}-factor of ~1.3, with that of ~0.8 prior to the transition. After the timing of 250 ms when the peak energy content is achieved, the energy content starts to decrease probably due to an increase in radiation loss, thus leading to radiation collapse before the end of the NBI pulse. There is a suggestion of impurity accumulation during the NBI-only H-mode phase, based on the growing rate of the AXUV signal as compared with the linear rise of line-averaged density.

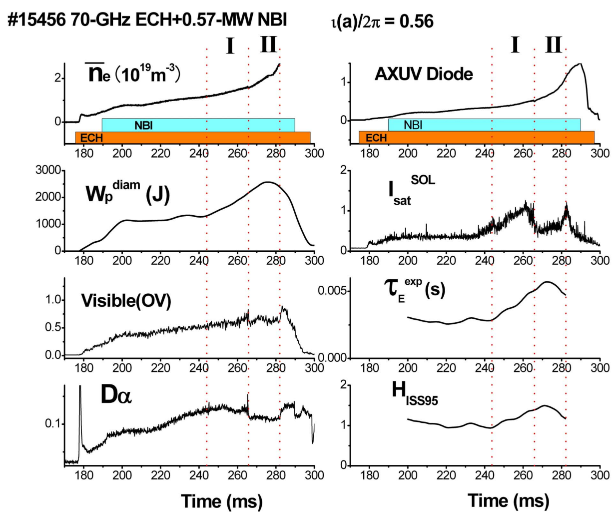

FIG. 3. Time evolution of the key plasma parameters for ECH(D^+)+NBI(H^0) plasma at $\iota(a)/2\pi$=0.56.

3.3. H-mode Transition of ECH (D^+) + NBI (H^0) Plasma

ECH has been overlapped with an NBI-sustained plasma. This type of plasma again shows a transition to H-mode. As Fig. 3 shows, because of the gradual nature of the H-mode transition (Phase I), it is a little difficult to identify the exact timing of the transition (~243ms) and hence to distinguish between L- and dithering H-mode phase. In Phase I, a gradual rise of $d\bar{n}_e/dt$ in the bulk plasma is seen while the substantial rise of dW_p^{diam}/dt can be seen. The detailed mechanism for this rise of plasma energy content is not yet understood. At the timing of 265 ms, a sharp drop of D_α is brought about with an established ELM-free H-mode. This H-mode phase (Phase II) is terminated by the back-transition to the L-mode which is indicated by a rapid recovery of the D_α signal back to its pre-H-mode level. The gain in τ_E^{exp}, i.e. $\Delta\tau_E^{exp}$, from the H-mode transition to the peak confinement time is about 4 ms and the H_{ISS95}-factor after the transition has achieved about 1.4 with that of ~1 prior to the transition.

4. Results of Experimental Analysis and Discussion

4.1. Configuration Dependence of H-mode Quality

Since the transition dynamics is expected to be linked with the specific magnetic structure, it is interesting to study how the peak H_{ISS95}–factor depends on the details of the magnetic configuration in Heliotron J. For simplicity, we here take up the peak value of the H_{ISS95}-factor as a key indicator of the achieved H-mode quality and the vacuum edge iota as a label of the operational configuration. Figure 4 shows the experimental iota dependence of (i) the peak H_{ISS95}-factor during the established H-mode phase and of (ii) the threshold H_{ISS95}-factor before the transition. It is found that some configurations show a remarkable improvement over L-mode (ISS95) confinement (1.3< H_{ISS95} <1.8) while others show only a slight improvement. For convenience of explanation, the iota range where the peak H_{ISS95}-factor reaches over 1.3 is shown as the hatching region. It is found that the hatching region is located in the iota range of slightly less than, but not on, the major natural resonances of n/m=4/8, 4/7, and 12/22. On the other hand, the experiments have revealed the presence of a weaker or modified version of the H-mode, the quality of which degrades as compared with that of the hatching region. In such a modified version of the H-mode, the D_α signal was found to show various types of behaviour at the transition, decreasing in some sections of the torus while increasing in other sections, depending on which plasma-wall interactions or gas dynamics the respective D_α monitors viewed in relation to the operational gas-puffing and neutral beam sources. Although the line-averaged density, the plasma energy content and the resultant energy confinement time rise with time, the improvement of the H_{ISS95} –factor during the H-mode is limited to be minor.

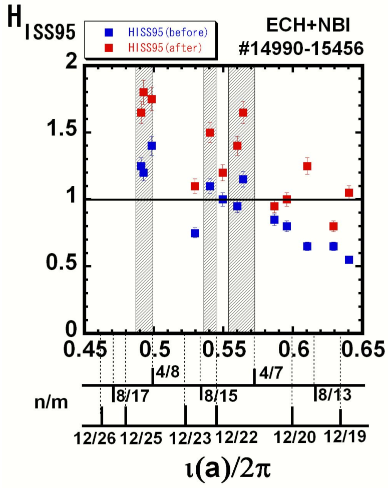

FIG.4. Edge iota dependence of the peak H_{ISS95}–factor after the H-mode transition (red) and the threshold H_{ISS95}-factor before the transition (blue) for ECH+NBI plasmas. The hatching shows the iota range of H_{ISS95} > 1.3.

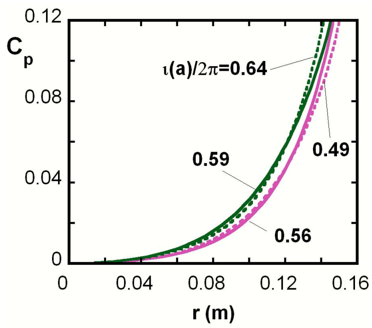

FIG.5. Poloidal viscous damping ratecoefficients at various configurations, the edge iotas of which are 0.49, 0.56, 0.59 and 0.64.

One of the key ingredients for the enhancement of the H-mode quality is expected to be the reduction of the poloidal viscous damping rate coefficient C_p=<$\mathbf{e}_p \cdot \nabla B/B$> in the outer plasma region [15, 16]. From the numerical configuration dependence of this damping rate coefficient C_p, it is found that there seems to be some coincidence between the enhancement of H_{ISS95}-factor and the reduction of C_p at r > 0.1 m, as shown in Fig.5. However, this result still remains inconclusive and further studies are needed.

4.2. Density Threshold of the H-mode Transition

In ECH and/or NBI plasmas, the line-averaged density is raised during the shot and then H-modes are observed only at densities higher than a certain threshold value. These H-mode discharges primarily explore the density threshold in the power vs density operating diagram. The power out-flux through the separatrix is expected to be the important quantity since the H-mode transition takes place at the plasma boundary. Figure 6-(a) and -(b) show such diagrams for those configurations which provide high-quality H-modes, $\iota(a)/2\pi$=0.56 and 0.49. Experiments have been carried out in the following three operation schemes: (i) ECH (D^+)-only plasmas with the injected ECH power of 0.12 to 0.39 MW, (ii) NBI-only plasmas with the injected NBI (H^0) power of 0.57 MW, and (iii) ECH (D^+) + NBI (H^0) combination plasmas with the injected NBI (H^0) power of 0.1 to 0.57 MW added by the ECH power of 0.29 MW. The results have revealed that no ECH-only H-mode transition occurs for the configuration of $\iota(a)/2\pi$=0.49 while the density threshold for ECH-only and ECH+NBI plasmas ($\bar{n}_e^{th}$ = 0.7 ~ $1.3\times10^{19}m^{-3}$) for the other configuration of $\iota(a)/2\pi$=0.56 is insensitive to the estimated input power absorption, P_{abs}, with regard to the start timing of Phase I. As for the timing of Phase II, a slight power dependence can be seen. It is noted that the density threshold for NBI plasmas ($\bar{n}_e^{th}$ ~$2.2\times10^{19}m^{-3}$) in the 2004 experimental campaign is a factor 2 higher than that of ECH or ECH+NBI plasmas. As a comparison, the density threshold for NBI plasmas in the 2003 campaign where the target plasma was provided by hydrogen ECH was in the range of 1~1.5×10^{19} m^{-3} and the density threshold differences among the various heating schemes were not significant. The reason for this difference between the 2003 and 2004 campaigns is not yet figured out, but there is a fair possibility that the H-mode density threshold depends on the history of plasma operation and vessel wall conditions. As for ECH+NBI plasmas, however, the marked difference of the density threshold throughout the 2002 and 2004 campaigns is not yet recognized. Under the 0.29-MW ECH and 0.57-MW NBI conditions, Figure 7 shows the configuration dependence of the density threshold (Phases I and II) at various iotas. It is found that there is a tendency of the lower density threshold at the timing of Phase II as well as Phase I to result in a larger enhancement of the ratio of the H_{ISS95}–factor after the transition to that before the transition.

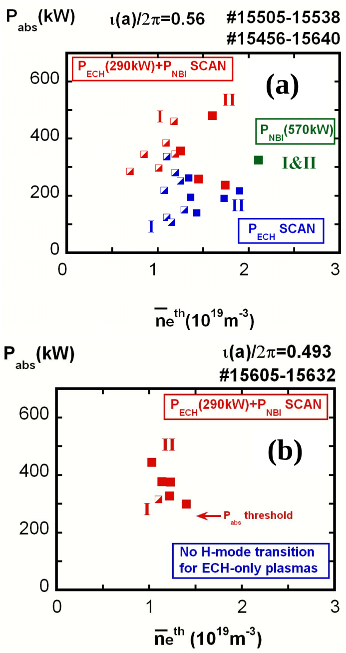

FIG.6. H-mode operataion window: heating power P_{abs}(kW) versus $\bar{n}_e^{th}$ ($10^{19}m^{-3}$)

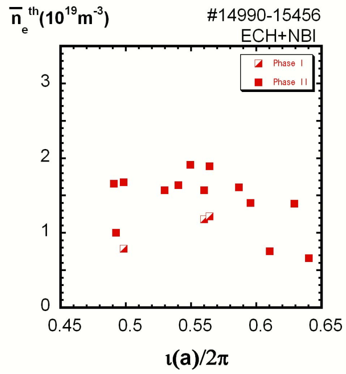

FIG. 7. Configuration dependence of the H-mode density threshold (Phases I and II).

4.3. Edge Plasma Characteristics at the H-mode Transition

The change of edge plasma was monitored with a Langmuir probe array located in the SOL. Four probe pins, which were aligned in one poloidal cross section of the torus, were used: the first pin with a fixed bias voltage for the ion-saturation current (I_s), the second and the third pins for floating potentials (V_f) at two positions and the fourth with 100 Hz scanning bias voltage for estimation of the electron temperature (T_e). Rapid changes in the ion-saturation current and the floating potential are also clearly observed at the H-mode transition of Phase II. Figure 8-(a) shows an example of the time evolution of the key plasma parameters as well as the ion-saturation current, I_s, at $R{-}R_{LCFS}$ = 27 mm, the measure of fluctuation induced particle flux, $\Gamma_{fluc.}$, estimated from the fluctuation components of the ion-saturation current and the floating potentials ($\Gamma_{fluc.} \propto \tilde{I}_s \times \left(\tilde{V}_f^1 - \tilde{V}_f^2\right)$); the positive value of $\Gamma_{fluc.}$ corresponds to the outward flow [17]. Here R is the radial position of the probe and R_{LCFS} is the radial position of the last closed flux surface calculated for the vacuum condition. At the timing of the rapid D_α drop (~248 ms), the I_s signal suddenly decreased while the fluctuation level, $I_{s,fluc.} = RMS\left(\tilde{I}_s - \bar{I}_s\right)/\bar{I}_s$, and the fluctuation induced flux $\Gamma_{fluct.}$ also decreased (Phase II). In this particular shot, the increase and the decrease in $\Gamma_{fluct.}$ were observed during 218 ms $\le t \le$ 248 ms in correspondence with the dithering of D_α signal. Sharp spikes with large amplitudes were observed in I_s, V_f and also in $\Gamma_{fluct.}$, indicating the intermittent nature of the edge plasma turbulence. After this H-mode transition, the apparent heights of the intermittent bursts seem to decrease but it is not clear whether their decreases indicate the change of the characteristic of the turbulence since their averaged values are also decreased after the transition.

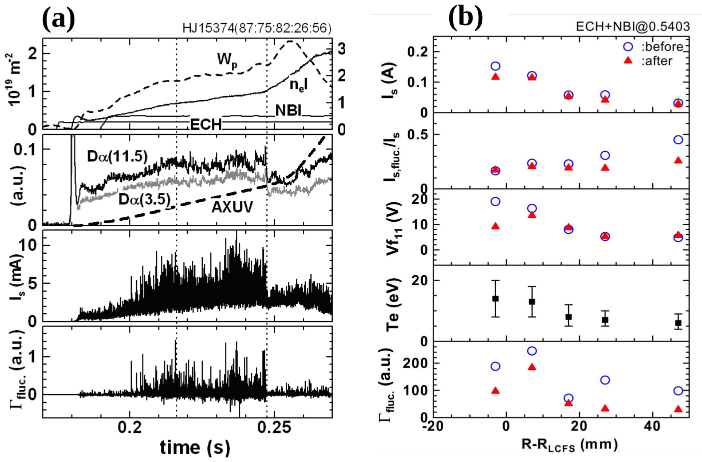

FIG.8. (a) Time evolution of $\bar{n}_e l$, W_p^{diam}, D_α signal, AXUV signal and I_s signal at R-R_{LCFC} = 27 mm and the fluctuation induced particle flux Γ_{fluc}. (b) Radial profiles of edge plasma parameters before and after the transition (~0.248 s).

Figure 8-(b) shows the radial distributions of I_s, $I_{s,fluc.}/I_s$, V_f, T_e and $\Gamma_{fluct.}$ before and after the transition on shot-by-shot basis. Due to the poor time resolution of T_e-measurement, the averaged T_e near the transition timing is plotted in this figure. Before the transition (~248 ms), the potential $V_f(R)$ increases with inserting the probe toward and beyond the last closed flux surface. On the other hand, the V_f-profile after the transition has a positive maximum at R-R_{LCFS} ≈10 mm. In order to study the effect of the radial electric field E_r on the plasma turbulence and resultant particle flux, the space potential (V_p) behaviour should be investigated instead of V_f. If we estimate the space potential V_p as V_f+3×T_e by ignoring a change of T_e through the transition, the drop of V_f near the last closed flux surface results in the formation of E_r-shear after the transition. For other field configurations and/or heating scenarios, however, such a change of V_f is not so clearly observed. Therefore, the detailed investigation of the relation between the formation of the E_r (or E_r-shear) and the edge plasma turbulence has just started.

5. Conclusion

The major goals of the Heliotron J program are obtaining an increased physics understanding of enhanced confinement modes and developing the concept and technology required to implement these understanding in the physics and engineering design of the optimized helical-axis heliotron. The experiments in the 2004 campaign have yielded information on a wide range of physics aspects of the H-mode, from the transition to well into the high-quality H-mode. Major results obtained from these areas of research are as follows:

(1) L-H transition studies of ECH(D^+)-only, NBI(H^0)-only and ECH+NBI combination heating plasmas have revealed the existence of the notable magnetic configuration dependence of the H-mode quality, supporting previous results in the 2002 campaign.
(2) The threshold line-averaged density, depending on the configuration, is in the region of $0.7\sim1.4\times10^{19}$ m^{-3} in ECH (0.29MW)+NBI (0.57MW) operation. The edge iota of the high-quality H-mode ($1.3< H_{ISS95} <1.8$) is located in the specific iota range of slightly less than the major natural resonances of n/m=4/8, 4/7, 12/22. The enhancement of H_{ISS95}-factor may be discussed in terms of the geometrical poloidal viscous damping rate coefficient C_p, but this remains inconclusive and further studies will be necessary.
(3) Edge plasma measurements suggest the reduction of the apparent heights of the intermittent bursts in the SOL density and the formation of the E_r (or E_r-shear) near the last closed flux surface at the transition. However, the detailed study has just started.

Finally, we need to continue to improve theory-experiment comparison to further improve understanding of the L-H transition in Heliotron J. In order to take this direction, the upgrades of the NBI system (<1.5 MW) and ICRF system (<1.0 MW) are now in progress.

Acknowledgement

The authors wish to thank the CHS/LHD teams at the National Institute for Fusion Science (NIFS) for their experimental contributions and helpful discussions. The work was performed with the support of Kyoto University 21st century COE Program as well as the NIFS Collaborative Research Program.

References

[1] SANO, F., et al., 30th EPS Conference on Contr. Fusion and Plasma Phys., St. Petersburg, 7-11 July 2003 ECA Vol.27A, O-2.2A.
[2] SANO, F., et al., J. Plasma Fusion Res.Vol.**79**, No.**11**(2003)1111.
[3] SANO, F., et al., 14th Intern. Stellarator Workshop, Greifswald, Germany, 21 September – 1 October 2003, paper No. I Tu.1.
[4] STROTH., U., et al., Nucl. Fusion, **36**(1996)1063.
[5] MIZUUCHI, T., et al., 14th Intern. Stellarator Workshop, Greifswald, Germany, 21 September – 1 October 2003, paper No. O.Tu 3.
[6] MIZUUCHI, T., et al., Plasma Science & Technology, Vol.**6**, No.4, Aug. 2004, p.2371.
[7] SANO, F., et al., Fusion Science and Technology, Vol.**46**, Sep. 2004, p.288.
[8] OBIKI, T., et al., Nucl. Fusion **44**(2004)47.
[9] KOBAYASHI, S., et al., in this conference.
[10] OBIKI, T., et al., Nucl. Fusion **41**(2001)833.
[11] WAKATANI, M., et al., Nucl. Fusion **40**(2000)569.
[12] SHIDARA, H., et al., Fusion Science and Technology, Vol.**45**, Jan. 2004, p.41.
[13] TRIBALDOS, V., et al., J. Plasma Fusion Res. **78**(2002)996.
[14] HANATANI, K., et al., Nucl. Fusion **32**(1992)1769. GASP., J, Research Report, Kyoto University, IAE-RR-2000-086. KANAME, H., Master Course Thesis, 2001.
[15] Wobig. H., et al., Plasma Phys. Control. Fusion **37**(1995)893.
[16] Hirsh, M., et al., "Plasma Phys. Control. Fusion **42**(2000)A231.
[17] Mizuuchi, T., et al., in the 16th PSI Conference (Portland, Main, May, 2004), to be published in J. Nucl. Mater.